

NUMERICAL INVESTIGATION ON THE MOTION OF 2-D PARTICLE CLOUDS

Xinya YING¹, Juichiro AKIYAMA², Masaru URA³

¹ Student Member of JSCE, Graduate Student, Graduate School of Engineering, Kyushu Institute of Technology
(1-1 Sensuicho, Tobataku, Kitakyushu 804-8550, Japan)

² Member of JSCE, Associate Professor, Dept. of Civil Engineering, Kyushu Institute of Technology

³ Member of JSCE, Professor, Dept. of Civil Engineering, Kyushu Institute of Technology

The motion of 2-D buoyant clouds formed by releasing fine particles into quiescent waters with finite depth is numerically studied. In the numerical model, particle phase is modeled by the dispersion model and turbulence is calculated by the large eddy simulation. The governing equations, including the filtered 2-D Navier-Stokes equations and mass transport equation, are solved based on the operator-splitting algorithm and an implicit cubic spline interpolation scheme. The eddy viscosity is evaluated by the modified Smagorinsky model including the buoyancy term. Comparisons of main flow characteristics, including shape, size, average buoyancy, moving speed and the amount of particles deposited on the bed, between experimental and computational results show that the numerical model well predicts the motion of the buoyant clouds in the whole process, from the falling to spreading stage. The effects of silt-fence on the motion of particle clouds are also investigated through numerical experiments.

Key Words : *buoyant cloud, particle, LES, Smagorinsky model, fluid-particle flow*

1. INTRODUCTION

Dumping dredged material, soil and rubble into coastal waters is often encountered in constructing man-made island and disposal of industrial waster etc. To predict diffusion of turbidity resulted from dumping such materials is of practical importance for assessing the environmental impact on plankton, benthic organisms and fishes near the disposal site.

The buoyant clouds formed by instantaneous releases of such materials, in particular, fine particles, fall under the action of their own buoyancy in initial times. After impinging on the bottom, the clouds spread horizontally. In this study, the motions of the clouds before and after the impingement are referred to as the falling stage and the spreading stage, respectively.

A number of studies on the falling stage of particle clouds have been performed. Nakatsuji et al.¹⁾ made a theoretical and experimental study on particle clouds and found that particle clouds behave like homogeneous counterparts if the initial volume is large and the particle size is relatively small. Buhler and Papantoniou²⁾ conducted a theoretical and experimental study on swarms of coarse

particles. They found that in the final stage, the front velocity remains constant and somewhat larger than the mean settling velocity of particles.

A few numerical investigations for the falling stage have been carried out. For example, Oda et al.³⁾ investigated the settling and spreading behavior of particle clouds using the improved DEMAC method. Li⁴⁾ studied particle clouds experimentally and numerically, and found that the velocity of the clouds approaches the terminal settling velocity of the individual particles and the growth rate of half width of clouds decreases with the magnitude of the settling velocity of particles.

In contrast to the investigations of the falling stage, only few studies have been performed on the spreading stage. Tamai et al.⁵⁾ extended the thermal theory to investigate the spreading stage of two-dimensional particle clouds formed by releasing a fixed volume of sand into waters with finite depth, and theoretically and experimentally found that the motion of particle clouds is dependent on the sand size. Tamai and Muraoka⁶⁾ qualitatively investigated turbidity transport produced by direct dumping of soil, using the two-fluid model. They found that the induced flow is depressed by slowing down the rate of dumping of soil.

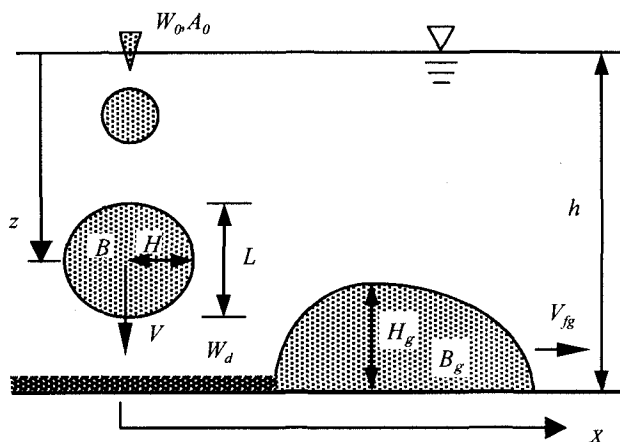


Fig. 1 Sketch of a particle cloud released into quiescent waters with finite depth

Table 1. Experimental conditions

Case	Matter to form cloud	s_p	d_{50} (mm)	ε_0	W_0 (m^3/s^2)
P1	Glass bead	2.47	0.044	0.194	0.00475
P2	Glass bead	2.47	0.088	0.124	0.00303
P3	Sand	2.65	0.140	0.194	0.00475
P4	Glass bead	2.47	0.044	0.200	0.00490
S1	Saline			0.200	0.00490

s_p = special gravity of particles; d_{50} = mean diameter of particles; $\varepsilon_0 = (\rho_0 - \rho_a) / \rho_a$

In this study, the motion of buoyant clouds formed by releasing fine particles into quiescent waters with finite depth is studied numerically. The dispersion model was chosen to model the particle phase. Turbulence is simulated by the large eddy simulation (LES). The validity of the numerical model is extensively tested against experimental data for the whole process of the motion of the particle clouds, from the falling to spreading stage. Comparisons of the main flow characteristics between the particle and the saline cloud are made as well.

2. EXPERIMENTS

The motion of a two-dimensional particle cloud, formed by instantaneously releasing a fixed volume of water-particle mixture into quiescent waters with finite depth, is schematically illustrated in Fig.1, in which W_0 = half total buoyancy force at initial point ($= A_0 g (\rho_0 - \rho_a) / \rho_a$); A_0 = half volume of the cloud per width at initial point; ρ_0 = initial density of the cloud; ρ_a = density of ambient fluid; h = water depth; H , L , B and V = half width, length, average buoyancy and mass center velocity of the cloud in the falling stage, respectively; H_g , B_g and V_{fg} =

height, average buoyancy and front propagation speed of the cloud in the spreading stage, respectively; W_d = buoyancy of deposited particles per unit length; W_s = total buoyancy of a particle cloud for the spreading stage.

As presented in Table 1, five cases of experiment were carried out in a glass flume of 7.5m length, 1.0m height and 0.1m width. The water depth in the glass flume was fixed at 0.9m. The particle clouds were formed by releasing glass beads for cases P1, P2 and P4, and sand for case P3. For case S1, the buoyant cloud was formed by releasing saline water. The whole process, from the falling to the spreading stage is studied in cases P4 and S1. Studies of other cases are limited to the falling stage only. In all cases, a fixed volume ($2A_0 = 0.005\text{m}^2$) of particle-water mixture or saline water was instantaneously released into waters by a device placed just above water surface.

The motion of the buoyant clouds was imaged by a VTR-camera moving with the buoyant clouds. The speed and the geometry of the clouds were obtained based on the analysis of the recorded images. To minimize the error, an experiment was repeated five times under the same conditions. The presented experimental results of the geometry and speed are average values of such five measurements. Average buoyancy of the falling stage B was calculated by assuming the conservation of total buoyancy. Average buoyancy of the spreading stage B_g for the saline cloud was estimated from the density distribution measured by conductivity meter and for the particle clouds from the mass of particles contained in the clouds, which is measured by separating a particle cloud using two slide gates and subsequently collecting the separated particles with a siphon tube. To obtain the profiles of B_g along distance, the measurements were carried out at five sections of different distances, repeating three times under the same experimental conditions for each section. The buoyancy of deposited particles per unit length W_d was determined by collecting the particles deposited to the bed with a siphon after suspended particles completely deposit to the bed. The experiment for measuring W_d was repeated three times under the same conditions. The experimental results of B_g and W_d presented in this work are the average values of three such measurements.

3. MODEL FORMULATION

In this study, the dispersion model was used to model particle phase. In the model, particle phase is treated as a continuous fluid and the drift velocity between fluid phase and particle phase is assumed to be the settling velocity of particles. This model is

efficient when particles are fine and dense, and was still successfully used, as in the numerical studies of convection of particle thermals by Li⁽⁴⁾ and sediment transport in open channel by Celik and Rodi⁽⁷⁾.

Applying the grid filter to the incompressible Navier-Stokes equations and mass transport equation, the governing equations for the mean-flow and mass transport are obtained⁽⁸⁾.

$$\frac{\partial U_i}{\partial x_i} = 0 \quad (1)$$

$$\frac{\partial U_i}{\partial t} + U_j \frac{\partial U_i}{\partial x_j} = -\frac{1}{\rho} \frac{\partial P}{\partial x_i} + \nu \frac{\partial^2 U_i}{\partial x_j^2} + \frac{\partial}{\partial x_j} (-\overline{u'_i u'_j}) + g_i \frac{\Delta \rho}{\rho} \quad (2)$$

$$\frac{\partial C}{\partial t} + (U_i + V_{si}) \frac{\partial C}{\partial x_i} = \frac{\partial}{\partial x_i} (-\overline{u'_i c'}) \quad (3)$$

where U_i = velocity component in the direction x_i ; P = pressure minus the hydrostatic pressure at reference density ρ_a ; ρ = density; $\Delta \rho$ = density excess ($= \rho - \rho_a$); g_i = specific body force in the direction x_i ; u'_i = fluctuating velocity; C = volume concentration of particles or dense fluid; c' = fluctuating concentration; $\overline{u'_i u'_j}$ = subgrid correlation terms between fluctuating velocity due to the grid-filtering; $\overline{u'_i c'}$ = subgrid correlation terms between fluctuating velocity and concentration; V_{si} = settling velocity of particles in the direction x_i .

$-\overline{u'_i u'_j}$ can be expressed as

$$-\overline{u'_i u'_j} = \nu_t \left(\frac{\partial U_i}{\partial x_j} + \frac{\partial U_j}{\partial x_i} \right) - \frac{2}{3} k \delta_{ij} \quad (4)$$

where ν_t = subgrid scale eddy viscosity; k = turbulent kinetic energy; δ_{ij} = Kronecker delta function. The last term in Eq. (4) represents the normal stresses and can be absorbed in the pressure terms of the momentum equations.

By assuming that subgrid turbulent production includes a buoyancy term^(8,9), ν_t is expressed as

$$\nu_t = (Cs \Delta)^2 \left(|\overline{S}|^2 - \frac{g_i}{\rho Sc_i} \frac{\partial \Delta \rho}{\partial x_i} \right)^{1/2} \quad (5)$$

where Δ = filter width, Cs = Smagorinsky constant, and $|\overline{S}| = (2\overline{S}_{ij}\overline{S}_{ij})^{1/2}$ = magnitude of large-scale strain rate tensor in which \overline{S}_{ij} is defined by

$$\overline{S}_{ij} = \frac{1}{2} \left(\frac{\partial U_i}{\partial x_j} + \frac{\partial U_j}{\partial x_i} \right) \quad (6)$$

The term $-\overline{u'_i c'}$ in Eq. (3) is generally assumed to be

$$-\overline{u'_i c'} = \frac{\nu_t}{Sc_i} \frac{\partial C}{\partial x_i} \quad (7)$$

where Sc_i = subgrid turbulent Schmidt number.

Eqs. (1), (2) and (3) are solved based on the operator-splitting algorithm and the Crank-Nicolson method-based cubic spline interpolation (CCS) scheme (see details in reference 10).

4. COMPUTATIONAL CONDITIONS

For cases P1, P2 and P3, the computational domain is a rectangle of 2.0m width and 1.4m height. All boundaries are considered as slip wall boundaries. The initial buoyant clouds have the same values of A_0 and W_0 as those in the experiments, centered at the centerline of the domain and 3 times of initial half width below water surface.

For cases S1 and P4, computational domain is a rectangle of 10.0m width and 0.9m height. The imposed boundary conditions for velocity, pressure and concentration are

$$V_\tau = 0, \quad V_n = 0 \quad (\text{bottom boundary})$$

$$\frac{\partial V_\tau}{\partial n} = 0, \quad \frac{\partial V_n}{\partial n} = 0 \quad (\text{side boundaries})$$

$$\frac{\partial V_\tau}{\partial n} = 0, \quad V_n = 0 \quad (\text{top boundary})$$

$$\frac{\partial P}{\partial n} = 0, \quad \frac{\partial C}{\partial n} = 0 \quad (\text{all boundary})$$

In the spreading stage, additional boundary condition is needed for the equation of mass conservation to describe the deposition of particles. In a sediment-laden open channel flow, the net-deposition rate D is commonly assumed to be proportional to free settling velocity V_s and near-bed reference concentration C_b . However, for general situations there is no accurate way to determine the net-deposition rate to the bed. Thus, we assume that D has an expression similar to that for a sediment-laden open channel flow, that is

$$D = \alpha V_s C_b \quad (8)$$

where α = empirical coefficient.

By matching experimental deposit with computational results, it is found that $\alpha = 2$ gives satisfactory results (Fig.9). The reason for $\alpha > 1$ is probably that the effective settling velocity of particles in turbulence is larger than the settling velocity of individual particle V_s . For example, Jobson and Sayre⁽¹¹⁾ have reported that for coarser sediment the effective settling velocity in turbulence is almost equal to V_s , but for finer sediment the effective settling velocity in turbulence is 1~2 times larger than V_s in their studies on suspended sediment transport in open channels.

In all cases, grid size was $0.01\text{m} \times 0.01\text{m}$. Time step size was 0.01s. The value of Cs was determined as 0.16, and the value of Sc_i as 0.1 for the saline cloud and 0.2 for the particle clouds so that good agreements between computational and experimental results for the falling stage are achieved. It is not surprising that there is a difference in the value of Sc_i between the saline and the particle clouds,

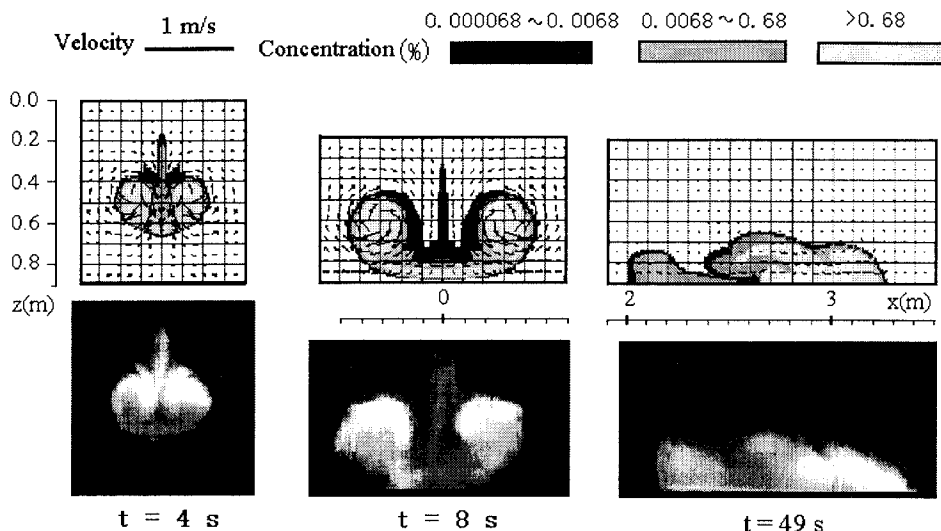


Fig.2 Photographs and computed velocity and density excess fields for case P4

because Sc_i depends on the local turbulence intensity and the molecular value Sc that varies with diffusing material¹²⁾. For the spreading stage, the same values of C_s and Sc_i as those for the falling stage are used.

Note that for convenience, the free water surface is treated as a horizontal rigid boundary in the computation. This treatment will be proved acceptable by comparing of computational results with experimental results in the next chapter.

5. NUMERICAL RESULTS

(1) Qualitative analyses

Photographs, computed concentration and velocity fields of the particle cloud for case P4 are shown in Fig.2. The figures at $t = 4$ s show the particle cloud in the falling stage. The figures at $t = 49$ s show the particle cloud in the spreading stage, subsequently formed after the impingement of the particle cloud on the bottom. $t = 8$ s is just before the impingement. It can be seen from these figures that shape, size and speed of the cloud are well simulated. It is demonstrated that the particle cloud, like a saline cloud¹⁰⁾, also has a wake and a flow-structure of two symmetrical vortices. Due to the entrainment of less dense ambient fluid into the central part from the rear of the cloud, a reverse mushroom shaped cloud is gradually formed ($t = 8$ s). After impingement, the cloud splits into two parts and each one propagates in the opposite direction along the horizontal bottom ($t = 49$ s). The flow becomes weaker with the distance, finally vanishing due to the settling of particles.

(2) Quantitative analyses for falling stage

In Figs.3~5, the computed results of non-dimensional half width H^* , average buoyancy B^* and

mass center velocity V^* for particle clouds are presented, along with those for the saline cloud, in which the non-dimensional quantities are defined as $x_f^* = x_f / A_0^{1/2}$; $H_g^* = H_g / A_0^{1/2}$; $B_g^* = B_g / (W_0 / A_0)$; $V_{fg}^* = V_{fg} / (W_0^2 / A_0)^{1/4}$; x_f = horizontal distance measured from the center of initial buoyant clouds to the front of horizontally spreading clouds. It is observed that the motion of the cloud composed of fine particles, that is, case P1 is well simulated and its H^* , B^* and V^* are close to that of the saline cloud. For case P2, in which the settling velocity of particles V_s is about 4 times larger than that in case P1, the reasonable agreements between the computational and the experimental results are achieved. For case P3, in which the settling velocity of particles V_s is about 10 times larger than that in case P1, the computed H^* , B^* and V^* significantly differ from the experimental results. From these comparisons, it may be roughly estimated that the present model is applicable if the settling velocity of particles remains less than 1/10 of the mass center velocity of the clouds.

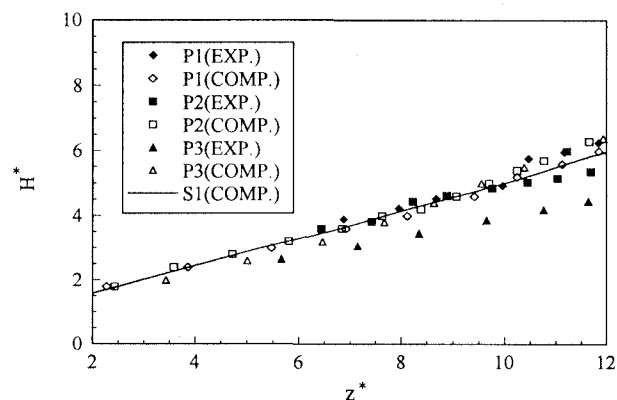


Fig.3 H^* as a function of z^*

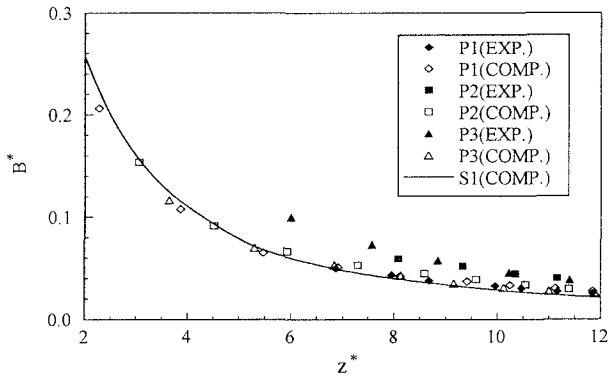


Fig.4 B^* as a function of z^*

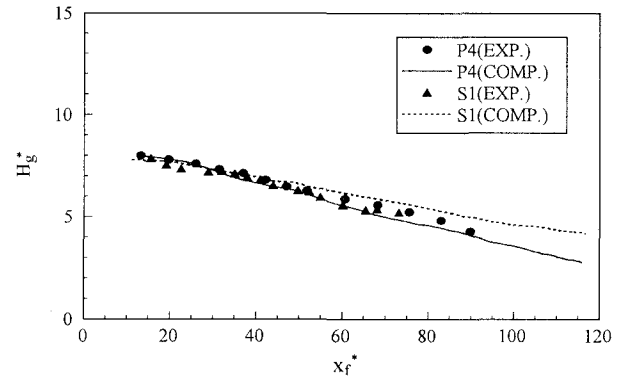


Fig.6 H_g^* as a function of x_f^*

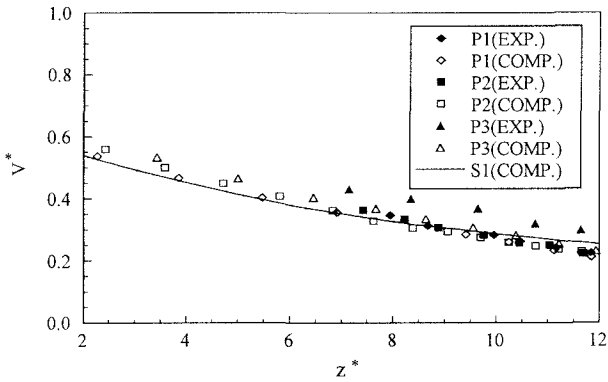


Fig.5 V^* as a function of z^*

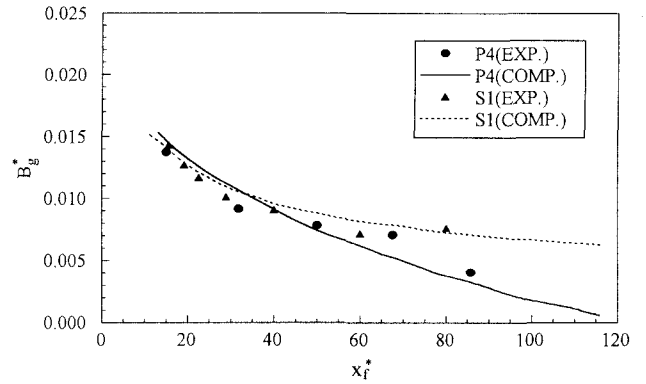


Fig.7 B_g^* as a function of x_f^*

(3) Quantitative analyses for spreading stage

In Figs.6~8, comparisons between computational and experimental results of non-dimensional height H_g^* , average buoyancy B_g^* and front propagation speed V_{fg}^* of the particle cloud and the saline cloud with the same W_0 are presented. It can be seen that H_g^* , B_g^* and V_{fg}^* are well predicted. These flow characteristics for the particle cloud decrease more rapidly with distance than the saline cloud because of settling of particles to the bed.

The buoyancy of deposited particles per unit length as a function of distance is presented in Fig.9, in which $W_d^* = W_d / (W_0 / A_0^{1/2})$. Both experimental and computed results show that the amount of deposit increases from a relatively small value at the impingement point to a maximum value at about $x^* = 46$ and then decrease towards zero. This deposit profile is formed because in the earlier times after the impingement, the circulating motion is relatively strong and most of the particles are in suspension, as shown in Fig.2 ($t=8s$). As the cloud moves forward, the motion becomes weaker, as shown in Fig.2 ($t=49s$), so that the deposition of particles increases.

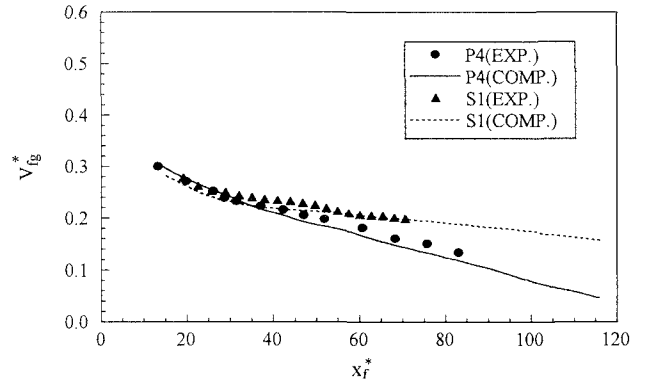


Fig.8 V_{fg}^* as a function of x_f^*

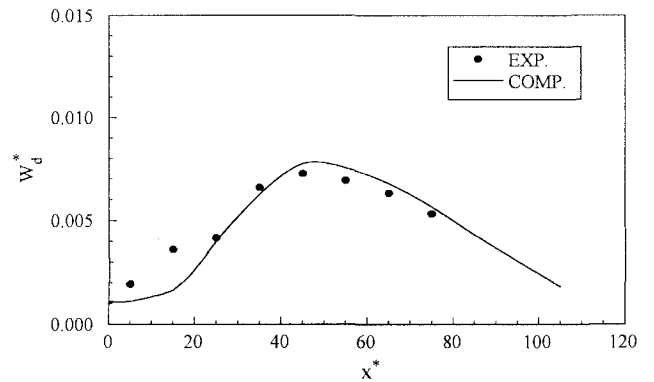


Fig.9 W_d^* as a function of x^* for case P4

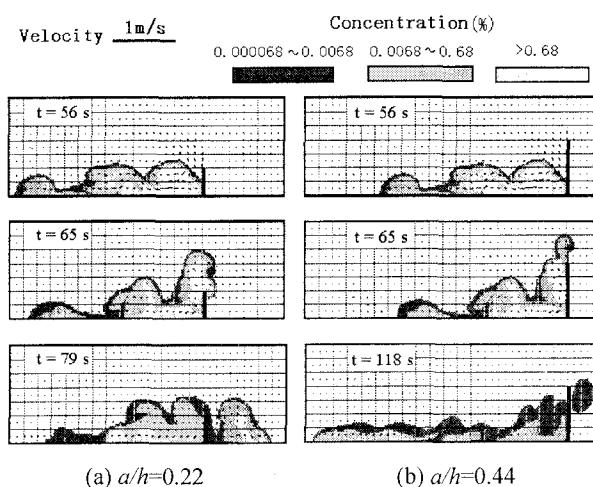


Fig.10 Motion of the particle cloud passing over silt-fences

6. EFFECTS OF SILT-FENCE ON THE MOTION OF PARTICLE CLOUDS

Silt-fences are widely used as an efficient tool in limiting diffusion of turbidity. To investigate the effects of silt-fence on the motion of particle clouds, two cases of numerical experiments are made. The computational conditions are the same as those of case P4. The silt-fence is placed at $L_s/h = 4$ and the height is $a/h=0.22$ and 0.44 , respectively, where L_s = horizontal distance between the releasing point and silt-fence; a = height of silt-fence.

Based on the computed results of case P4, if there is no silt-fence, the amount of particles passing the position where the silt-fence is placed is about 31% of W_0 . If there is a silt-fence and $a/h=0.22$, part of the cloud can pass over the silt-fence, as shown in Fig.10a, and its amount is about 8% of W_0 . When $a/h=0.44$, the particle cloud is almost limited inside the silt-fence, as shown in Fig.10b. The computed results show that the silt-fence can efficiently prevent the diffusion of turbidity.

7. CONCLUSIONS

(1) For the falling stage:

(a) If the settling velocity of particles V_{st} remains less than 1/10 of the mass center velocity V of the particle clouds, the numerical model with $C_s=0.16$ and $Sc_t=0.2$ can well predict the motion of the particle clouds.

(b) For the cloud composed of finer particles, the variations of non-dimensional half width H^* , average buoyancy B^* and mass center velocity V^* with non-dimensional distance z^* are close to those of the saline cloud.

(2) For the spreading stage:

(a) The numerical model can well predict the non-dimensional height H_g^* , average buoyancy B_g^* ,

front propagation speed V_{fg}^* and buoyancy of deposited particles W_d^* with the same values of C_s and Sc_t as those in the falling stage.

(b) The non-dimensional height H_g^* , average buoyancy B_g^* , front propagation speed V_{fg}^* of the particle cloud decrease more rapidly with non-dimensional distance x^* than those of the saline counterpart, because of settling of particles.

(c) The numerical model is possible to simulate complex motion of the particle clouds passing over the silt-fence.

ACKNOWLEDGMENT: This study was supported by the Grant-in-Aid for Science Research of the Ministry of Education and Culture, Japan under the Grant B(2), No.08455232.

REFERENCE

- 1) Nakatsuji, K., Tamai, M. and Murota, A.: Dynamic behaviors of sand clouds in water, *Int. Conf. Phys. Modelling of Transport and Dispersion*, M.I.T. Boston, 8C.1-8C.6, 1990.
- 2) Buhler, J. and Papantoniou, D.A.: Swarms of coarse particles falling through a fluid, *Proc. of Int. Symposium on Environmental Hydraulics*, Vol.1, pp.135-140, 1991.
- 3) Oda, K., Shigematsu, T. Onishi, N. and Inoue, M.: Numerical simulation of settling and spreading behavior of particle cloud using improved DEMAC method, *Proceedings of Coastal Engineering*, JSCE, Vol.39, pp.971-975, 1992 (in Japanese).
- 4) Li, C.W.: Convection of particle thermals, *Journal of Hydraulic Research*, IAHR, Vol.35, No.3, pp.363-376, 1997.
- 5) Tamai, M., Muraoka, K., Murota, A. and Machida, H.: Study on initial stage of diffusion process of turbidity in direct dumping of soil, *Journal of Hydraulic, Coastal and Environmental Engineering*, JSCE, No.515/II-31, pp.77-86, 1995 (in Japanese).
- 6) Tamai, M. and Muraoka, K.: Numerical simulation on characteristics of turbidity transport generated in direct dumping of soil, *Annual Journal of Hydraulic Engineering*, JSCE, Vol.42, pp.541-546, 1998 (in Japanese).
- 7) Celik, I. and Rodi, W.: Modeling suspended sediment transport in nonequilibrium situations, *Journal of Hydraulic Engineering*, ASCE, Vol.114, No.10, pp.1157-1191, 1988.
- 8) Ying, X.: Motion of buoyant cloud released into quiescent waters with finite depth, Doctoral Thesis, Kyushu Institute of Technology (in press).
- 9) Eidson, T. M.: Numerical simulation of the turbulent Rayleigh-Benard problem using subgrid modeling, *J. Fluid Mech.*, Vol.158, pp.245-268, 1985.
- 10) Ying, X., Akiyama, J. and Ura, M.: Motion of dense fluid released into quiescent water with finite depth, *Journal of Hydraulic, Coastal and Environmental Engineering*, JSCE, No.635/II-49, pp.141-152, Nov. 1999.
- 11) Jobson, H.E. and Sayre, W.W.: Vertical transfer in open channel flow, *J. Hydr. Engrg.*, ASCE, 96(HY3), pp.703-724, 1970.
- 12) Reynolds, A.J.: The prediction of turbulent Prandtl and Schmidt numbers, *Int. J. Heat Mass Transfer*, Vol.18, pp.1055-1069, 1975.

(Received September 30,1999)